Proceedings of the Canadian Society for Mechanical Engineering International Congress 2021
CSME Congress 2021
June 27-30, 2021, Charlottetown, PE, Canada

EXPERIMENTAL INVESTIGATION OF THE EFFECT OF COMPLIANCE PROPERTIES ON THE FLOW IN AN ANALOGOUS EX-VIVO HEART PERFUSION SYSTEM

Guilherme M. Bessa[1], Jake Hadfield[1], Hyun-Joong Chung[2], Reza Sabbagh[1], Darren H. Freed[3], David S. Nobes[1*]
[1]Department of Mechanical Engineering, University of Alberta, Edmonton, AB, Canada
[2]Department of Chemical and Materials Engineering, University of Alberta, Edmonton, AB, Canada
[3]Department of Surgery, Physiology & Biomedical Engineering, University of Alberta, Edmonton, AB, Canada
*dnobes@ualberta.ca

Abstract—The heart transplant waiting list far exceeds supply. This shortage is generally attributed to the high number of discarded hearts and to the narrow six-hour time window currently available through the standard preservation method: static cold storage (SCS). An alternative method called ex-vivo heart perfusion (EVHP) maintains a human donor heart beating outside the body for the time preceding transplantation surgery. By keeping the heart working in a physiologically consistent way and monitoring its functions, the organ's health can be assessed and the transplant time window can be extended. In order to improve and optimize the EVHP system, the present work aims to further investigate the relationship between pulsatile flow and compliance by assessing the effect of different compliant tubes on the upstream and downstream pressure and flow fields. Hence, silicone tubes of variable compliance, length, and geometrical shape were developed for this study — although only one sample has been tested so far, in addition to an experimental setup containing a hydraulic circuit analogous to the left flow loop of the EVHP system. The flow fields downstream of the compliant section are assessed using laser Doppler velocimetry (LDV). Findings will include novel visualizations of these flow fields as well as comparisons of pressure waveforms from an assortment of compliance conditions.

Keywords- cardiovascular flow; aorta; ex vivo heart perfusion; pulsatile flow; shadowgraph; LDV

I. INTRODUCTION

The number of patients awaiting heart transplantation is much higher than the supply [1] [2]. Many reasons exist for the low supply, and it is generally attributed to three factors: high disposal rate among available donor hearts [1] [3], the narrow six-hour window currently available through the standard preservation method —static cold storage (SCS) [4], and the non-use of hearts categorized as being of extended donor criteria (ECD) and donation after circulatory death (DCD) [5] [6]. In view of this, many donated hearts are not used. Many patients, especially those who live geographically far from major transplant centers, are as a result unable to donate or receive any heart. To better coordinate the demand for organ transplants with the supply, the donor pool must be expanded.

Pursuant of the goal to increase the pool of donor hearts, a novel surgical procedure called ex-vivo heart perfusion (EVHP) has been proposed as an alternative and most promising method to perform heart transplants. By keeping the heart beating while being transported from the donor to the recipient patient, EVHP technology allows the organ's health to be assessed and the transplant time window can be extended [7]-[9]. The latest improvements in EVHP systems enable the heart to work in a quasi-physiological regime [1], [10]-[17]. Here, the perfusate — a solution made of blood and nutrients [15] —, is pumped into the left side of the heart, which is periodically electrically stimulated to produce contraction in a physiological working mode. In this way, by monitoring the metabolic and mechanical responses of the heart in response to the imposed downstream conditions, it is possible to measure cardiac performance and provide the medical team with valuable information that allows them to better assess the viability of the transplant [2]-[5]. In fact, a recently published study shows that online monitoring of the heart's functional parameters is the most effective way to assess the organ's health [1]. It can be said that such control of the heart's metabolism to keep it healthy is well understood and continues to be optimized [1], [10]-[17]. However, the fluid mechanics intrinsic to the EVHP system, and the corresponding impact on cardiac performance, still need to be better investigated.

The EVHP flow loop mimics the human cardiovascular system, which consists of two loops in parallel: the pulmonary and systemic vessel networks. The latter is mainly characterized by the compliant structure of the aorta and, i.e. by the fluid-structure interaction responding to the unsteady effects of the pulsatile flow [18]. However, such aorta compliance feature is not currently involved in the EVHP system because its hydraulic circuit is essentially composed of rigid tubes. In a previous work, it was shown that the use of a compliant tube, mimicking the aorta, instead of a rigid tubing

in the EVHP system's flow loop could alter the flow-pressure relationship of the pulsatile flow, making it more similar to the physiological profile and also reducing the workload of the heart [19]. However, this study was conducted with only a single compliant tube. The effects of different parameters, such as tube geometry and material, have not yet been investigated before this work.

In order to improve and optimize the EVHP system, the present work aims to further investigate the relationship between pulsatile flow and compliance by assessing the effect of different designs of compliant tubes on the upstream and downstream pressure and flow fields. To this end, silicone tubes of variable compliance, length, and geometrical shape were developed for this study, in addition to an experimental setup containing a hydraulic circuit analogous to the systemic flow loop of the EVHP system. Findings will include novel visualizations of these flow fields as well as comparisons of pressure waveforms from the most assorted compliant cases.

A. *Literature review*

The effort required to ensure blood flow throughout the body is provided by the heart in its process of contraction and relaxation [20]. Cardiac performance is generally assessed by interpreting the pressure waveform in peripheral arteries [21]. In clinical trials, the pressure waveform is recognized as an important marker for cardiovascular health due to the non-invasive nature of such measurement. However, to obtain more accurate information about the general conditions of the cardiovascular system, it is necessary to assess the pressure waveform within the aorta [22]. An extended overview of the human cardiovascular system can be found in standard textbooks on physiology [23], [24].

The theory about pulsatile flow is well-founded [18], [25]-[27]. In a remarkable study from 1955 [25], Womersley proposed a method to characterize and quantify a pulsatile flow in a straight circular tube. The resultant dimensionless quantity, Womersley number (α), correlates the unsteady and viscous effects of a pulsatile flow:

$$\alpha = \frac{D}{2}\sqrt{\frac{\rho\omega}{\mu}} \tag{1}$$

where D is the tube inner diameter [m], ρ is the fluid density [kg/m3], μ is the fluid viscosity [Pa·s] and ω is the pulse frequency [rad/s]. In the aorta human aorta, α usually ranges from 12-20 ([18], [28], [29]).

Mathematical modeling, numerical simulations and experimental investigations of pulsatile flow regimes in rigid tubes are well developed [30]-[32]. Nevertheless, these approaches are limited from a physiological perspective due to the elastic response of the aorta, which can expand in a range of 20-60% during the systolic phase of the cardiac cycle [33], storing up to 50% of the volume of fluid ejected from the left ventricle (LV) [34]. Right after the systole, the LV recovery phase (diastole) begins. At this point, the aortic valve closes and the aorta contracts. This elastic function, in addition to inducing blood perfusion in the arterial tree during diastole, helps to reduce pressure pulsations in peripheral vessels. Such compliant behavior is also known as the Windkessel effect [34].

There are several clinical trials focused on the wave-propagation phenomenon [35] and experimental studies of flow fields in low α regimes through compliant models [36] - [38], but there are few ex-vivo experimental studies that take into account the effects of aortic compliance on the flow fields in a near-physiological regime.

B. *Current EVHP System*

The current EVHP setup taken as a reference [19] in this work is shown in Fig. 1. The system is composed of a reservoir, two centrifugal pumps, arterial filter, oxygenator and a tubing network connecting all devices to the heart. Pump P1 supplies perfusate to the left atrium (LA) and right atrium (RA), and the heart, stimulated by a pacemaker, contracts and pumps the fluid forward. Pump P2 is responsible for providing back pressure to the heart by pumping against the direction of ventricular outflow, simulating the vascular afterload. The flows coming from the LV and the Pump P2 mix and then pass through the oxygenator, to immediately join the flow that comes from the RV and return to the reservoir. Pressure and flow are monitored at strategic points in the flow loop, providing constant feedback on heart conditions. The region of interest in the present study, the left flow loop of the EVHP system, is highlighted in red in Fig. 1.

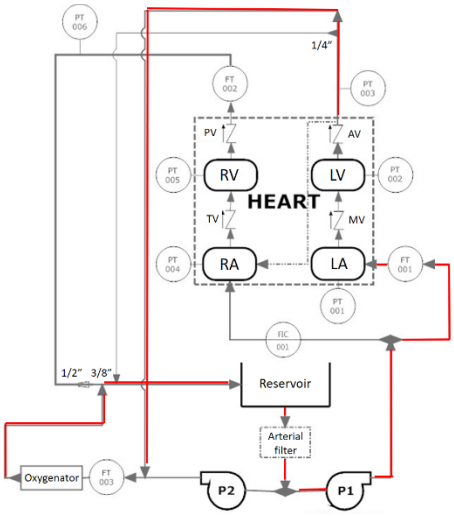

Heart	
LA	Left Atrium
MV	Mitral Valve
LV	Left Ventricle
AV	Aortic Valve
RA	Right Atrium
TV	Tricuspid Valve
RV	Right Ventricle
PV	Pulmonary Valve

EVHP System	
FIC	Flow Indicating Controller
FT	Flow Transmitter
PT	Pressure Transmitter

Figure 1. Schematic of the current EVHP system. The region of interest in the present study, the left flow loop, is highlighted in red. Figure modified from [19].

II. METHODOLOGY

A. *Experimental steup*

A schematic representation of the experimental setup is shown in Fig. 2. The mechanical flow loop analogous to the EVHP system has two regions of interest. The first one, the

imaging section, was a mock aorta contained in a pressure chamber. The second region, where the velocity data is acquired with LDV, is a 3/4" ID (inner diameter) quartz glass tube surrounded by a sealed chamber with a 1/16" thick quartz window for allow laser access. To prevent laser diffraction, this chamber was filled with quartz glass' refractive index matched fluid: 58% of water potassium thiocyanate (KSCN) solution. A pulsatile waveform is generated using a computer-controlled mechanical diaphragm pump (ARC® PX05), which ejects flow through a custom-moulded tri-leaf exit valve to simulate the physiological working condition of the heart. The diaphragm pump is driven by a CNC stepper motor (Teknic® CPM-SCSK-3441S-ELSA), which in turn is controlled by a C++ code. Thus, the flow generated by the pump can be precisely regulated. The pump ejection phase is based on *in-vivo* measurements of a real cardiac stroke volume; 70 mL/cycle [24]. The experimental flow loop was also equipped with an afterload pump (Jostra Rotaflow RF-32 Centrifugal Pump) to control the back pressure of the system. However, the preliminary case discussed here did not have any back pressure applied.

An image acquisition system was set up to monitor the tube response throughout the pump cycle. The camera (Basler Pioneer®, Basler Vision Technologies) has a resolution of 648 × 488 pixels and was used to capture images at a frame rate of 200 fps. Images were collected in a shadowgraph mode with a LED backlight illumination. The field of view was positioned at the midpoint of the tube length. The pressure-chamber in the present case was maintained at atmospheric pressure.

Pressure transducers (Edwards® Truwave Disposable Pressure Transducers) were installed at the entrance and exit of both the mock aorta and the diaphragm pump. The pressure data was acquired at a sample rate of 4 kHz. For the preliminary case investigated in the present study, the diaphragm pump was adjusted to 60 BPM (1 Hz). Therefore, considering the physical properties of the working fluid (water), ρ = 1000 kg/m^3 and μ = 8.9 x 10^{-4} Pa.s, the Womersley number becomes 25, which is just above the physiological range 12-20 ([18], [28], [29]). Of note, future tests will be carried out with another working fluid to bring the Womersley number into the appropriate range. The pressure waveform, the mock aorta images, and the trigger signal from the camera were collected with an in-house built code (LabWindows CVI, National Instruments). Images of the mock aorta were processed through an in-house developed code (Matlab, The Mathworks Inc.) used to identify tube walls and then calculate the tube diameter in each image.

B. Mock aorta

The compliant tubes are in-house manufactured using a 3D SLA printer (Form2, FormLabs Inc.) to generate the external moulds and the tubular skeletal support structures, as shown in Fig. 3, followed by silicone casting (Ecoflex™ 00-50 or Dragon Skin™ 10). Several compliant tubes have been designed and are under development, including different skeletal patterns. However, at the current stage of the project, only one sample has been tested: a silicone tube made of Ecoflex™ 00-50 without any internal support structure (skeleton). The compliant tube used here is 19 mm inner diameter, 4 mm thick and 100 mm long. The casting process is briefly depicted in Fig. 3.

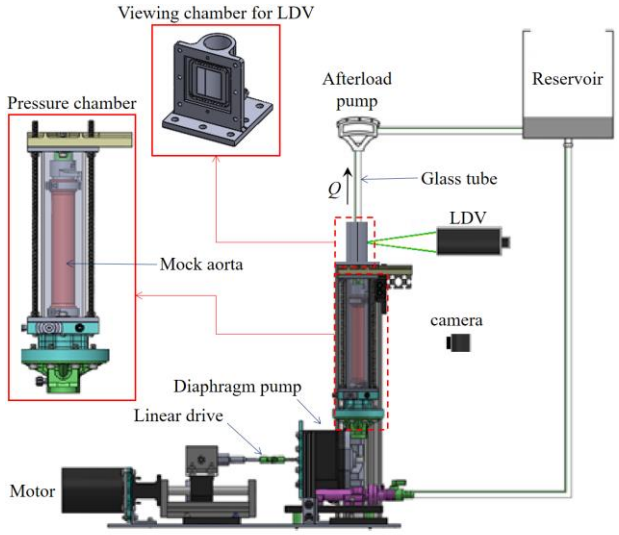

Figure 2. Schematic of experimental setup. The zoomed views show the pressure chamber and the viewing chamber for the LDV.

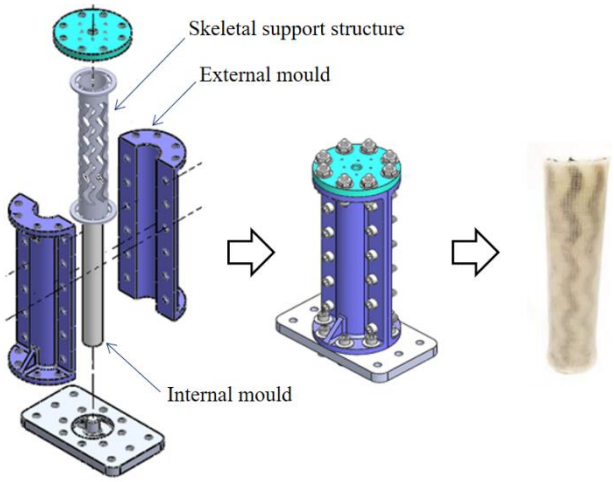

Figure 3. Mock aorta casting process. On the left, the exploded view, followed by the isometric view of the mould assembly and on the right, the casted silicone model.

III. RESULTS

The results presented in this section are preliminary and were obtained with only one model of mock aorta. Also, no back pressure was applied using the afterload pump or pressure in the pressure-chamber. The latter remaining at atmospheric pressure.

Fig. 4 presents the pressure waveform measured at the mock aorta outlet (blue) over one normalized pump cycle. For comparison and reference purposes, a typical physiological pressure waveform from human ascending aorta [39] — the arterial region just above the left ventricle outlet —, and the pump cycle are also represented. In the latter, depicted by the

dashed line, it can be seen that the ejection phase (systole) occurs approximately in the first third of the cycle, when the curve reaches its peak, followed by the recovery phase (diastole), which occurs in the remaining two thirds. Here, the key parameters under evaluation are the peak systolic pressure, P_S, the diastolic pressure, P_D, both the position and the pressure level of the valley, P_V, and, ultimately, the ratio between the lengths of the systolic and diastolic phases. When comparing both curves, the pressure measured experimentally in the system with the physiological reference [39], it can be observed that both reach similar peak values (P_S), around 16 kPa, and practically in the same phase of the cycle (~ 0.25 s). However, in the pump recovery regime, the pressure curve measured in the system differs considerably from the physiological profile. The experimental pressure curve presents a more accentuated valley than the physiological profile, reaching values of approximately 6 kPa (~ 0.4 s), which most resembles a local minimum and does not significantly change the trend of the curve. It is noteworthy that this valley on the pressure curve, also known as the dichrotic notch, is a response to the closing of the aortic valve and characterizes the end of fluid ejection during the systolic phase. In the sequence, a second pressure peak is observed, which is more prominent and delayed in the experimental curve, reaching values around 11.5 kPa (~ 0.6 s). This second peak, which occurs when there is no fluid supply from the pump, is thought to be due to the oscillation of the interaction of the elastic tube with the mass of the contained fluid. In addition to differing in profile, the difference from the systolic and diastolic pressure levels ($P_S - P_D$) of the current experimental pressure curve is much greater than that observed in physiological profiles. Future tests will alter some experimental parameters, such as the back pressure from the afterload pump, the pressure level inside the pressure-chamber, and the geometric characteristics of the mock aorta in order to approximate the experimental pressure waveform to the physiological profile.

Fig. 5 represents the maximum distension of mock aorta along the pump cycle. The percentage values were calculated taking as reference the dimensions of the tube under the load of only the water column in the system, approximately 1 m. As can be seen, the mock aorta distention has two peaks, as well as in the pressure curve. The first one, which occurs in the systolic phase, is due to the pump ejection and reaches 15%. The second, which occurs in the diastolic phase, as explained above it is thought to be due to the oscillation of the elastic tube wall and reaches approximately 5%. The contribution of pulse pressure is slightly below to the desired physiological range, which can vary from 20-60%, depending on several factors, i.e. patient's health and age.

Next, Fig. 6 shows the axial component of the velocity measured at the centerline of the tube from selected phase-averaged of 10 pump cycles. Measurements were taken at a point 120 mm downstream of mock aorta using the LDV system. Following trends in the pressure and tube distension curves, the streamwise velocity component also presents two peaks. The first, which occurs in the systolic phase, is due to the ejection of fluid from the pump and reaches 0.4 m/s. The second, which occurs in the diastolic phase, again it is thought to be due to the oscillation of the elastic tube wall and reaches approximately 0.2 m/s. To further assess the flow fluid, Fig. 7 shows the velocity profiles across the tube diameter at phases 120°, 180°, 300° and 350° of the pump cycle, as indicated by the letter A, B, C and D respectively on the dashed line in Fig. 6. As can be seen, the first phase (A) was chosen randomly in the ejection phase (systole), the second one (B) coincides with the first peak of the curve and the third (C) with the minimum value in the diastolic phase and the fourth (D) with the second peak. Altogether, 18 data points make up the profile, each point 1 mm apart, resulting from selected phase-averaged of 10 pump cycles. An important observation here is that the flow was relatively symmetrical throughout almost the entire cycle, as can be seen in Fig. 7. However, it is worth noting a slight asymmetry during the flow deceleration, evident in the backflow near to the walls — more accentuated in the left wall of the tube (see the red line Fig. 7). This backflow is consistent with Womersley's modeling of pulsatile flow in rigid tubes [25].

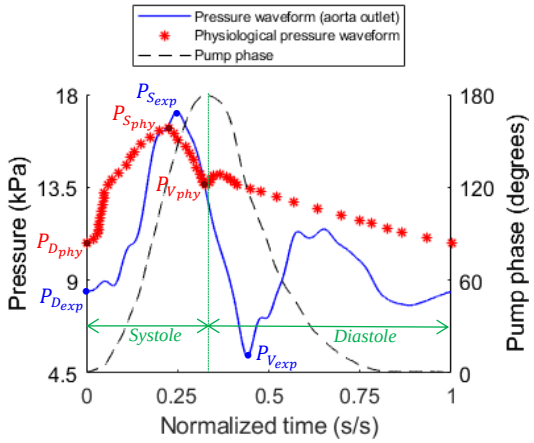

Figure 4. Pressure waveform at mock aorta outlet (blue) over one normalized pump cycle (dashed line). Diaphragm pump frequency at 1 Hz. Physiological pressure waveform in red [39].

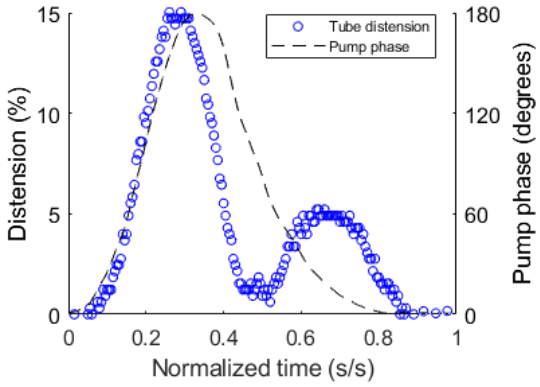

Figure 5. Tube distension over one normalized pump cycle (dashed line). Diaphragm pump frequency at 1 Hz.

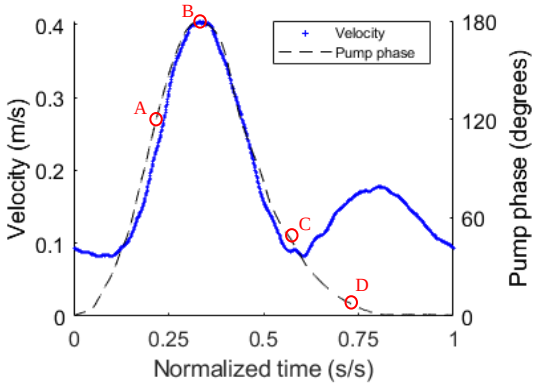

Figure 6. Flow velocity (axial component) measured at the center line of the tube over one normalized pump cycle (dashed line). Diaphragm pump frequency at 1 Hz.

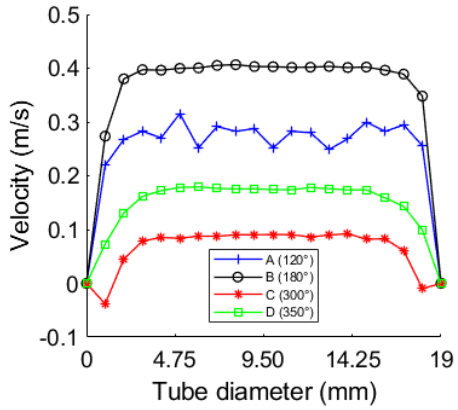

Figure 7. Velocity profile (axial component) across tube diameter at pump phase: A (120º) in blue; B (180º) in black; C (300º) in red and D (350º) in green. Diaphragm pump frequency at 1 Hz.

IV. CONCLUSIONS

This paper is part of an ongoing study that aims to improve an EVHP System. Of particular interest, this research is focused on investigating the effect of tube compliance on the downstream pressure and flow fields. The pressure waveforms, centerline velocity data and velocity profiles were combined with the mock aorta distention over a normalized pump cycle. Shadowgraph imaging was used to monitor the tube response over the pump cycles. For the only mock aorta tested up to this point, the maximum distension record was 15%, just below the physiological range. The pressure waveform acquired at the mock aorta outlet shows that, although the measured systolic pressure coincides with the physiological data, the diastolic phase profile is still quite different from the physiological profile taken as a reference here. A key observation regarding the velocity data was the presence of backflow in the flow deceleration phase, evidencing Womersley's theory for rigid tubes. It is expected from future tests, varying the mock aorta geometry and material, to be able to better assess which quantities play the major roles in the flow fields to ultimately optimize and improve the EVHP system.

ACKNOWLEDGMENT

This study has being conducted with the support of the Natural Sciences and Engineering Research Council (NSERC) of Canada, the Canadian Foundation of Innovation (CFI), the Canadian National Transplant Research Program (CIHR/CNTRP) and the University Hospital Foundation (UHF).

REFERENCES

[1] C. W. White et al., "Assessment of donor heart viability during ex vivo heart perfusion," Can. J. Physiol. Pharmacol., vol. 901, no. May, pp. 893–901, 2015.

[2] S. Messer, A. Ardehali, and S. Tsui, "Normothermic donor heart perfusion: Current clinical experience and the future," Transpl. Int., vol. 28, no. 6, pp. 634–642, 2014.

[3] S. J. Messer et al., "Functional Assessment and Transplantation of the Donor Heart Following Circulatory Death," J. Hear. Lung Transplant., 2016.

[4] J. F. McAnulty, "Hypothermic organ preservation by static storage methods: Current status and a view to the future," Cryobiology, vol. 60, no. 3 SUPPL., pp. S13–S19, 2010.

[5] D. H. Freed and C. W. White, "Donor heart preservation: straight up, or on the rocks?," Lancet, vol. 385, no. 9987, pp. 2552–2554, 2015.

[6] S. M. Minasian, M. M. Galagudza, Y. V. Dmitriev, A. A. Karpov, and T. D. Vlasov, "Preservation of the donor heart: from basic science to clinical studies," Interact. Cardiovasc. Thorac. Surg., vol. 20, no. 4, pp. 510–519, 2015.

[7] D. H. Rosenbaum, M. Peltz, M. E. Merritt, J. E. Thatcher, H. Sasaki, and M. E. Jessen, "Benefits of Perfusion Preservation in Canine Hearts Stored for Short Intervals," J. Surg. Res., vol. 140, no. 2, pp. 243–249, 2007.

[8] S. Repse, S. Pepe, J. Anderson, C. McLean, and F. L. Rosenfeldt, "Cardiac reanimation for donor heart transplantation after cardiocirculatory death," J. Hear. Lung Transplant., vol. 29, no. 7, pp. 747–755, 2010.

[9] M. J. Collins, S. L. Moainie, B. P. Griffith, and R. S. Poston, "Preserving and evaluating hearts with ex vivo machine perfusion: an avenue to improve early graft performance and expand the donor pool," Eur. J. Cardio-thoracic Surg., vol. 34, no. 2, pp. 318–325, 2008.

[10] C. White et al., Impact of Myocardial Load on the Preservation of Donor Heart Function during Ex Vivo Perfusion, vol. 35. 2016.

[11] C. W. White *et al.*, "Avoidance of Profound Hypothermia during Initial Reperfusion Improves the Functional Recovery of Hearts Donated after Circulatory Death," *Am. J. Transplant.*, vol. 16, no. 3, pp. 773–782, 2016.

[12] C. White et al., Ex vivo perfusion in a loaded state improves the preservation of donor heart function, vol. 31. 2015.

[13] C. W. White *et al.*, "A cardioprotective preservation strategy employing ex vivo heart perfusion facilitates successful transplant of donor hearts after cardiocirculatory death.," *J. Heart Lung Transplant.*, vol. 32, no. 7, pp. 734–43, 2013.

[14] C. White, J. Nagendran, and D. Freed, Assessment of Preload-Recruitable Stroke Work During Biventricular Ex Vivo Heart Perfusion: A Novel Approach Eliminating The Pressure-Volume Loop Catheter. 2015.

[15] C. W. White *et al.*, "A whole blood-based perfusate provides superior preservation of myocardial function during ex vivo heart perfusion.," *J. Heart Lung Transplant.*, vol. 34, no. 1, pp. 113–21, 2015.

[16] S. Hatami *et al.*, "Endoplasmic Reticulum Stress in Ex Vivo Heart Perfusion: a Comparison Between Working Versus Non-Working Modes," *Can. J. Cardiol.*, vol. 33, no. 10, p. S68, 2017.

[17] C. White et al., Impact of Reperfusion Calcium and pH on the Resuscitation of Hearts Donated After Circulatory Death, vol. 103. 2016.

[18] D. N. Ku, “Blood Flow in Arteries,” *Annu. Rev. Fluid Mech.*, vol. 29, pp. 399–434, 1997.

[19] K. Cameron, M. E. Hassan, R, Sabbagh, D. H. Freed, D. S. Nobes, “Experimental investigation into the effect of compliance of a mock aorta on cardiac performance”, *Journal of Biomechanical Engineering*, vol. 15, no. 10, pp. 1-24, 2020.

[20] R. M. Berne, B. M. Koeppen, and B. A. Stanton, Berne & Levy Physiology. Philadelphia: Mosby/Elsevier, 2003.

[21] M. E. J. Bridges, “Monitoring Arterial Blood Pressure: What You May Not Know,” vol. 22, no. 2, 2002.

[22] C.-H. Chen et al., “Estimation of Central Aortic Pressure Waveform by Mathematical Transformation of Radial Tonometry Pressure,” Circulation, vol. 95, no. 7, p. 1827 LP-1836, Apr. 1997.

[23] A. C. Guyton, Textbook of Medical Physiology. Philadelphia: Saunders. 1967.

[24] W. F. Boron, E. L. Boulpaep, Medical Physiology. Amsterdam: Elsevier, 2003

[25] J. R. Womersley, “Method for the calculation of velocity, rate of flow and viscous drag in arteries when the pressure gradient is known.,” J. Physiol., 1955.

[26] N. B. Wood, “Aspects of fluid dynamics applied to the larger arteries.,” J. Theor. Biol., vol. 199, no. 2, pp. 137–161, 1999.

[27] W. E. Langlois and M. O. Deville, Slow Viscous Flow. 2014.

[28] J. D. Bronzino, The Biomedical Engineering Handbook 1, 2nd Editio. New York: Springer Science & Business Media, 2000.

[29] A. F. Stalder et al., “Assessment of flow instabilities in the healthy aorta using flow-sensitive MRI,” J. Magn. Reson. Imaging, vol. 33, no. 4, pp. 839–846, 2011.

[30] G. Pontrelli, “Pulsatile blood flow in a pipe,” Comput. Fluids, vol. 27, no. 3, pp. 367–380, 1998.

[31] [37] M. Zácek and E. Krause, “Numerical simulation of the blood flow in the human cardiovascular system.,” J. Biomech., vol. 29, no. 1, pp. 13–20, 1996.

[32] [38] C. A. Taylor and M. T. Draney, “Experimental and Computational Methods in Cardiovascular Fluid Mechanics,” Ann. Phys. (N. Y)., vol. 36, pp. 197–231, 2004.

[33] [39] L. Huetter, P. H. Geoghegan, P. D. Docherty, M. S. Lazarjan, D. Clucas, and M. Jermy, “Application of a meta-analysis of aortic geometry to the generation of a compliant phantom for use in particle image velocimetry experimentation,” in IFAC-PapersOnLine, 2015, vol. 48, no. 20, pp. 407–412.

[34] G. G. Belz, “Elastic properties and Windkessel function of the human aorta.,” Cardiovasc. Drugs Ther., vol. 9, no. November 1993, pp. 73–83, 1995.

[35] P. Segers, J. Mynard, L. Taelman, S. Vermeersch, and A. Swillens, “Wave reflection: Myth or reality?,” Artery Res., vol. 6, no. 1, pp. 7–11, 2012.

[36] R. Yip, R. Mongrain, and A. Ranga, “Development of anatomically correct mock-ups of the aorta for PIV investigations,” no. 1, pp. 1–10, 2011.

[37] P. H. Geoghegan, N. A. Buchmann, C. J. T. Spence, S. Moore, and M. Jermy, “Fabrication of rigid and flexible refractive-index-matched flow phantoms for flow visualisation and optical flow measurements,” *Exp. Fluids*, vol. 52, no. 5, pp. 1331–1347, 2012.

[38] D. M. Amatya and E. K. Longmire, “Simultaneous measurements of velocity and deformation in flows through compliant diaphragms,” J. Fluids Struct., vol. 26, no. 2, pp. 218–235, 2010.

[39] F. N. Vosse, N. Stergiopulos,” Pulse Wave Propagation in the Arterial Tree”, Annual Review of Fluid Mechanics, vol. 43, no. 1, pp. 467-499, 2011